Stabilization of Therapeutic Proteins

Jhih-Wei Chu[1], Jin Yin[2], Oleg. A. Mazyar[3], Lin-Tang Goh[4], Miranda G. S. Yap[5], Daniel.I.C. Wang[6], and Bernhardt. L. Trout[7]

[1]Graduate Student, Department of Chemical Engineering, MIT
[2]Research Scientist, Department of Chemical Engineering, MIT
[3]Research Scientist, Department of Chemical Engineering, MIT
[4]Research Fellow, Bioprocessing Technology Center, NUS
[5]Director, Bioprocessing Technology Center, NUS and Department of Chemical & Environmental Engineering, NUS
[6] Institute Professor and Department of Chemical Engineering, MIT; Temasek Professor, NUS
[7]Assistant Professor, Department of Chemical Engineering, MIT
e-mail: jwchu@mit.edu, yin_jin@mit.edu, oamazyar@mit.edu, btcGohLT@nus.edu.sg, : cheyapm@nus.edu.sg, dicwang@mit.edu, trout@mit.edu

***Abstract*—We present results of molecular simulations, quantum mechanical calculations, and experimental data aimed towards the rational design of solvent formulations. In particular, we have found that the rate limitation of oxidation of methionine groups is determined by the breaking of O-O bonds in hydrogen peroxide, not by the rate of acidic catalysis as previously thought. We have used this understanding to design molecular level parameters which are correlated to experimental data. Rate data has been determined both for G-CSF and for hPTH(1-34).**

***Index Terms*—protein stabilization, excipients, molecular simulations, kinetics.**

I. Introduction

OXIDATION is a significant chemical modification for organic and biological compounds[1,2]. Peroxides, including hydrogen peroxide, hydroperoxides, and peroxy acids are efficient oxidants in a variety of solvents[3]. For example, oxidation of methionine groups by peroxides is a major degradation pathway for therapeutic proteins. Designing a storage formulation to provide an acceptable shelf-life is one of the most challenging tasks in the process of drug development[4-6]. The oxygen transfer from hydroperoxides to the nucleophilic substrates in solution is generally accepted as a S_N2 type displacement (eq.(1)) reaction[3,7]:

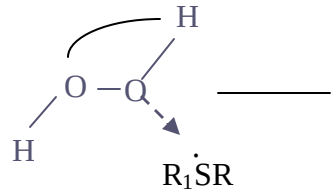

$$\longrightarrow R_1SOR_2 + H_2O \quad (1)$$

Thus, the transfer of oxygen is thought to be associated with a hydrogen shift to the distal oxygen. Typical observed activation barriers for peroxide oxidation of amines and organic sulfides in aqueous solutions are in the range of 10-20 kcal/mol[3,7-9]. Since the direct 1,2 hydrogen transfer of H_2O_2 in vacuum has a very high energy barrier (56 kcal/mol) [10], solvent molecules must have strong stabilization effects on the reaction to have the observed activation energies[11]. The acid-catalyzed mechanism (eq.(2)) is generally accepted as the mechanism for peroxide oxidation[12,13], where HA is a general acid and it can be a solvent molecule. In eq.(2), the general acid serves as a intermediate agent for the hydrogen transfer. Experimental evidences supporting the acid-catalyzed mechanism include the increase of oxidation rates with solvent pK_a and the change of reaction order of hydrogen peroxide

Manuscript received November 8, 2002. This work was supported in part by the Singapore MIT Alliance.

Bernhardt L. Trout, corresponding author, is with the Massachusetts Institute of Technology, Department of Chemical Engineering, Cambridge, MA, 02139 USA (phone: 1-617-258-5021; fax: 1-617-258-5042; e-mail: trout@mit.edu).

Jhih Wei Chu is with the Massachusetts Institute of Technology, Department of Chemical Engineering, Cambridge, MA, 02139 USA (e-mail: jwchu@mit.edu).

Jin Yin is with the Massachusetts Institute of Technology, Department of Chemical Engineering, Cambridge, MA, 02139 USA (e-mail: yin_jin@mit.edu).

Oleg A. Mazyar is with the Massachusetts Institute of Technology, Department of Chemical Engineering, Cambridge, MA, 02139 USA (e-mail: oamazyar@mit.edu).

Lin-Tang Goh is with the Bioprocessing Technology Center at the National University of Singapore, Singapore 119260 (e-mail: btcGohLT@nus.edu.sg).

Miranda G. S. Yap is with the Bioprocessing Technology Center and the Department of Chemical & Environmental Engineering at the National University of Singapore, Singapore 119260 (e-mail: cheyapm@nus.edu.sg).

Daniel I. C. Wang is with the Massachusetts Institute of Technology, Institute Professor and Department of Chemical Engineering, Cambridge, MA, 02139 USA; His is also the Temasek Professor at NUS (e-mail: dicwang@mit.edu).

from one in polar solvents to two in non-polar media[12], where the peroxide molecule plays the role of the general acid.

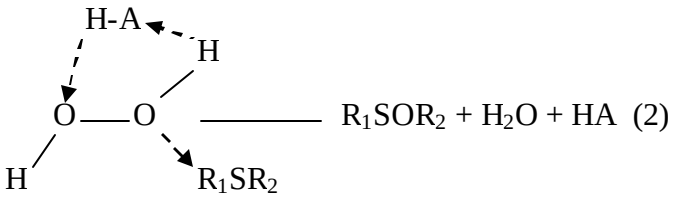

$$\longrightarrow R_1SOR_2 + H_2O + HA \quad (2)$$

Ab initio calculations on the acid-catalyzed mechanism have been performed for both the hydrogen transfer reaction of hydrogen peroxide[10,14] and for oxidation of amines and sulfides with hydrogen peroxide[10,11,15]. The attempt is to develop a mechanistic understanding of the oxidation mechanism. Important issues include the roles of the general acid, the order by which the transfer of oxygen and hydrogen proceeds, and the predicted activation energies. A correct mechanism must predict an activation barrier corresponding to experimental measurements (10-20 kcal/mol) [3,7-9]. Base on eq.(1) and eq.(2), three mechanisms have been studied[10,11,15]. The first is based on eq.(1), with the 1,2 hydrogen transfer to the distal oxygen occurring after the break of O-O bond. The leaving group is the solvated hydroxyl ion(OH^+). This type of ionic mechanism has been found for the oxidation of ammonia[11] by methyl hydroperoxide and the oxidation of trimethylammine[15] by hydrogen peroxide in the presence of a water molecule. The second mechanism is based on eq.(2). The rate-limiting step is the transfer of hydrogen to the distal oxygen to form an active form of hydrogen peroxide, water oxide[10,11]. The transfer of oxygen from the solvated water oxide to the nucleophile occurs afterwards. The third mechanism is also based on eq.(2) except that the transfer of hydrogen occurs after the break of O-O bond, and the rate-limiting step is the transfer of oxygen atom to the nucleophile. In both cases, the general acid involves in the reaction as a hydrogen transfer intermediate. For the above three mechanisms, the calculated activation barriers in previous studies are in the range of 28-50 kcal/mol, unreasonably higher than experimental data (10~20 kcal/mol). [10,11,15] Therefore, it was concluded that the general acid along can not catalyze the oxidation reaction[11]. On the other hand, when both a protonated solvent and a general acid catalyst are involved, the calculated energy barriers lie in between 5-15 kcal/mol, in agreement with experiments[11] (eq.(3)).

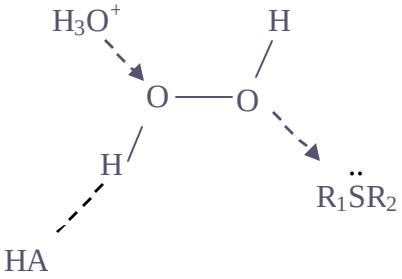

$$\longrightarrow R_1SOHR_2 + 2H_2O + HA \quad (3)$$

A protonated solvent is involved, and the reaction rate is suggested to decrease with pH by this mechanism.

The pH dependence of the oxidation rates of dimethyl sulfide (DMS) [16]and the methionine residues in human parathyoid hormone[17] have been measured. In the range between pH=2 to 10, oxidation rates of DMS with H_2O_2 in aqueous solutions are nearly constant, an increase in oxidation rates was observed only when pH is below 2. Therefore, the mechanism proposed by Bach et al (eq.(3)) may occur at very low pH values. PH-independent oxidation rates were also observed in various pH ranges for the oxidation of DMS in different types of solvent[16]. Methionine oxidation by hydrogen peroxide of human parathyroid hormone[17] was also found to have pH independent rates between pH=2 and pH=8 for both Met8 and Met18. In general, experimental observations do not indicate pH dependence of peroxide oxidation between low (pH=2-5) and high (pH=7-10) pH values. Therefore, it is important to resolve the underlying oxidation mechanisms over these pH ranges.

Further motivation for this study can be seen in the results in Figure 1. Here, it can be seen clearly that the activity of the protein decreases as the methionine groups in the protein are oxidized.

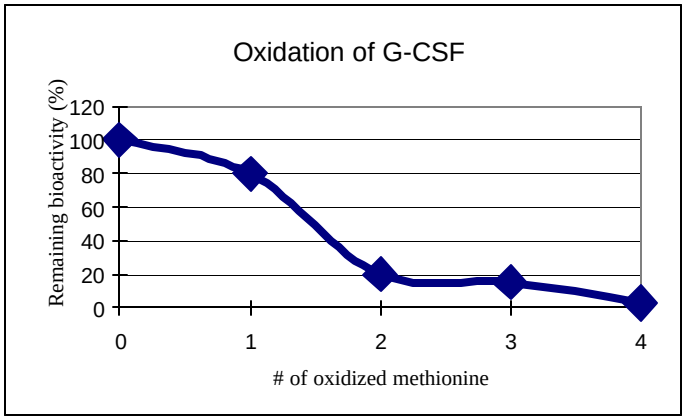

Fig. 1. Bioactivity as a function of the number of methionine residues oxidized.

In this study, we analyze the peroxide oxidation mechanisms by high level ab initio simulations. Both the hydrogen transfer reaction of H_2O_2 and the oxidation reaction of dimethyl sulfide were studied. Solvent effects including explicit configurations of water molecules and implicit electrostatic polarization were also investigated. The goal is to develop a theoretical mechanism of peroxide oxidation with activation barriers and pH-dependence in agreement with experimental observations.

II. METHODOLOGY

A. Quantum Calculations

Ab initio calculations were performed using the GAUSSIAN 98 package[18]; B3LYP (Becke's three-parameter

functional[19]) with the 6-31++G(d,p) basis set was employed for geometry optimizations, transition-state searches and frequency calculations throughout this study; a scaling factor of 0.9806[20] was used for zero-point-energies (ZPEs) corrections. All transition states reported have only one imaginary vibrational mode without imposing constraints during the process of geometry optimization. The polarized continuum model[21,22], PCM, was used to describe the long-range electrostatic polarization of the surrounding environment. Water is the only solvent considered (ε_r=80), and the united atom topological model[23] was used to build up the solute cavity.

To test if the B3LYP functional can properly address the calculational difficulties involved in the 1,2 hydrogen transfer reaction of hydrogen peroxide[10] (eq (4)), geometries of hydrogen peroxide, the transition-state, and water oxide were fully optimized at B3LYP, MP2[24,25] and CCSD[26,27] levels of theories with the 6-31++G(d,p) basis set. The B3LYP calculations predict accurate geometries compared with the CCSD results. For all calculations with the B3LYP functional, water oxide has lower energies than the transition state; thus have qualitatively current behavior compared to the Hartree-Fock calculations[10]. The MP2 SCF correlation correction on the B3LYP/6-31++G(d,p) geometries (58.32 kcal/mol for $\Delta E_1^{\ddagger}$ and 7.93 for $\Delta E_2^{\ddagger}$) greatly improves the agreement with the MP2/6-31++G(d,p)//MP2/6-31++G(d,p) results (57.944 kcal/mol for $\Delta E_1^{\ddagger}$ and 7.798 for $\Delta E_2^{\ddagger}$) . Both $\Delta E_1^{\ddagger}$ and $\Delta E_2^{\ddagger}$ at the MP2/6-31++G(d,p) //B3LYP/6-31++G(d,p) calculations also agree well with the CCSD/6-31++G(d,p) results (54.61 kcal/mol for $\Delta E_1^{\ddagger}$ and 8.71 for $\Delta E_2^{\ddagger}$). A sensitivity test of energy barriers to the number of basis functions at the MP2 theory also indicates that the 6-31++G(d,p) basis functions predict accurate barrier heights compare to larger basis functions, including 6-31++G(3df,3dp), cc-pVDZ and aug-cc-pVDZ. However, using the 6-31G(d) basis functions predicts a too high value of $\Delta E_1^{\ddagger}$ and a too low value of $\Delta E_2^{\ddagger}$. In conclusion, the geometry optimized at the B3LYP/6-31++G(d,p) level with an MP2 post-SCF correlation correction can provide satisfactory geometries and energetics for H_2O_2 chemistry, and thus, this approach is used throughout this study.

B. Molecular Simulations

Molecular dynamics simulations of G-CSF and of hPTH(1-34) were performed using the CHARMM package. The CHARMM22 all-atom potential was used to describe the energy function of proteins. The initial structure of G-CSF was obtained from x-ray crystallographic data found in the PDB and that of hPTH(1-34) was obtained from the NMR studies of Marx et al (PDB entry 1ZWA). As coordinates of all hydrogen atoms in histidine residues were reported for the HSD isomeric structures only, coordinates of hydrogen atoms for HSE and HSP structures were generated using the HBUILD function of CHARMM. 100 steepest descent steps followed by 500 conjugate gradient steps with the restraint force constant of 20 kcal/mol/A applied to heavy atoms were performed on the initial protein structures to optimize the position of the imidazole hydrogen atoms. This procedure was repeated with the restraining force constant of 10 kcal/mol/A to further optimize the imidazole rings for the HSE and protonated HSP structures of histidine. The resulting protein structures have 0.04 A root-mean-square deviation (RMSD) from the corresponding NMR structures and were used as the reference in analysis.

The reference structures were then solvated in a pre-equilibrated truncated octahedral water cell containing 5255 water molecules with a lattice length of 60 A. Water molecules with positions of oxygen atoms within 2.6 A to heavy protein atoms were removed resulting in a cell containing only 4986 water molecules. To balance the charge of the protein molecule, counter Na^+ and Cl^- were placed using the SOLVATE program, minimizing electrostatic forces on the cell walls. 200 steepest descent followed by 800 conjugate gradient minimization steps with all atoms unconstrained were performed to optimize solvated structures of protein. Energy of these cells were used as one of the factors affecting the choice of the optimal NMR structure of hPTH(1-34).

The selected systems were then heated up to 295 K by gradually scaling velocity (3K/0.1 ps) for 10 ps. Cutoff radius for electrostatic interactions was 15 A. Periodic boundary conditions were applied and the long-range Coulombic interactions were calculated using the particle-mesh Ewald summation method. Covalent bonds were fixed using the SHAKE algorithm during the dynamics simulation thus allowing the a 0.002 ps integration time step. During the 10 ps heating period, the heavy atoms of hPTH(1-34) fragment were restrained to the reference structure by a force constant of 10 kcal/mol/A. During the 30 ps equilibration period following after the heating period, the restraint force constant for heavy protein atoms was gradually decreased by 5 kcal/mol/A to 0 every 10 ps. For the last 10 ps of equilibration of the system and following phase of the molecular dynamics calculations, the Nose-Hoover thermostat was applied to control the cell temperature around 295 K.

Molecular dynamics simulations were performed for three protonated states of hPTH(1-34). The first state corresponds to the high pH case (pH = 7) with only one of the nitrogen atom in the imidazole ring of histidine residues protonated. In the second case, corresponding to the medium range of pH (pH = 5), both nitrogen atoms of imidazole rings are protonated. The last case corresponds to the low pH case (pH = 3), with both the nitrogen atoms of histidine residues and carboxyl oxygens of aspartic and glutamic acids residues protonated. 2 ns molecular dynamics simulations were performed for selected NMR structures of hPTH(1-34) at different pH conditions.

C. Experiments

1) Oxidation of proteins

G-CSF (supplied by Amgen, Inc.) and hPTH (1-34) (Sigma P-3796) were incubated with H_2O_2 (Sigma H-1009) in the pH range of 2-8 at 25 ^oC [final H_2O_2 concentration = 1 mM, hPTH (1-34) concentration = 40 μM]. Incubation buffers used were 50 mM phosphate for pH 2, citrate for pH 4 and pH

6 and Tris for pH 8. The ionic strengths of all buffers were adjusted to 0.2 M with the supplement of NaCl. At various time intervals, oxidation was terminated by loading samples onto a high pressure liquid chromatography (HPLC).

2) Separation of oxidized forms

Oxidized forms were separated by reverse-phase HPLC. The apparatus used was a Beckman Coulter System Gold® HPLC system (USA) that includes a type 126 solvent module, a type 168 detector and a type 508 autosampler. 30 µl H_2O_2-oxidized sample was injected into a C_4 column (Vydac 214TP52; 300 Å, 5 µm, 2.1 mm i.d. × 25 cm). The mobile phases used were solvent A (0.1% (w/v) trifluoroacetic acid (TFA)) and solvent B (0.1% (w/v) TFA in 90% acetonitrile). The column was initially equilibrated with 20% B at a flow rate of 0.2 ml/min. After sample injection, the separation was performed by a linear gradient of 20% B to 28% B for 10 min and 28% B to 35% B for 70 min at a flow rate of 0.2 ml/min with the UV detector set at 215 nm.

3) Mass spectrometry

Matrix-assisted laser desorption/ionization time-of-flight mass spectrometry (MALDI-TOF MS) was performed at the MIT Biopolymers Laboratory, using a Voyager-DE™ STR BioSpectrometry Workstation (PerSepctive Biosystems). Sample was dried in a Speed-Vac first and then purified with $ZipTip_{C18}$ (Millipore) following the manufacturer's instruction. α-Cyano-4-hydroxycinnamic acid was used as matrix. Measurement was made in the positive, linear mode and the accelerating voltage was 20000 V.

III. RESULTS AND DISCUSSION

The oxidation mechanism can be seen in Figure 2. The bar on the upper left side, to the right of the transition state structure demonstrates the charge as a function of position along the reaction trajectory. The water molecule included in the reaction trajectory helps to stabilize the charge of the intermediates. As can be seen in the figure, proton transfer does not occur until after the oxygen-oxygen bond has been stretched to the breaking point.

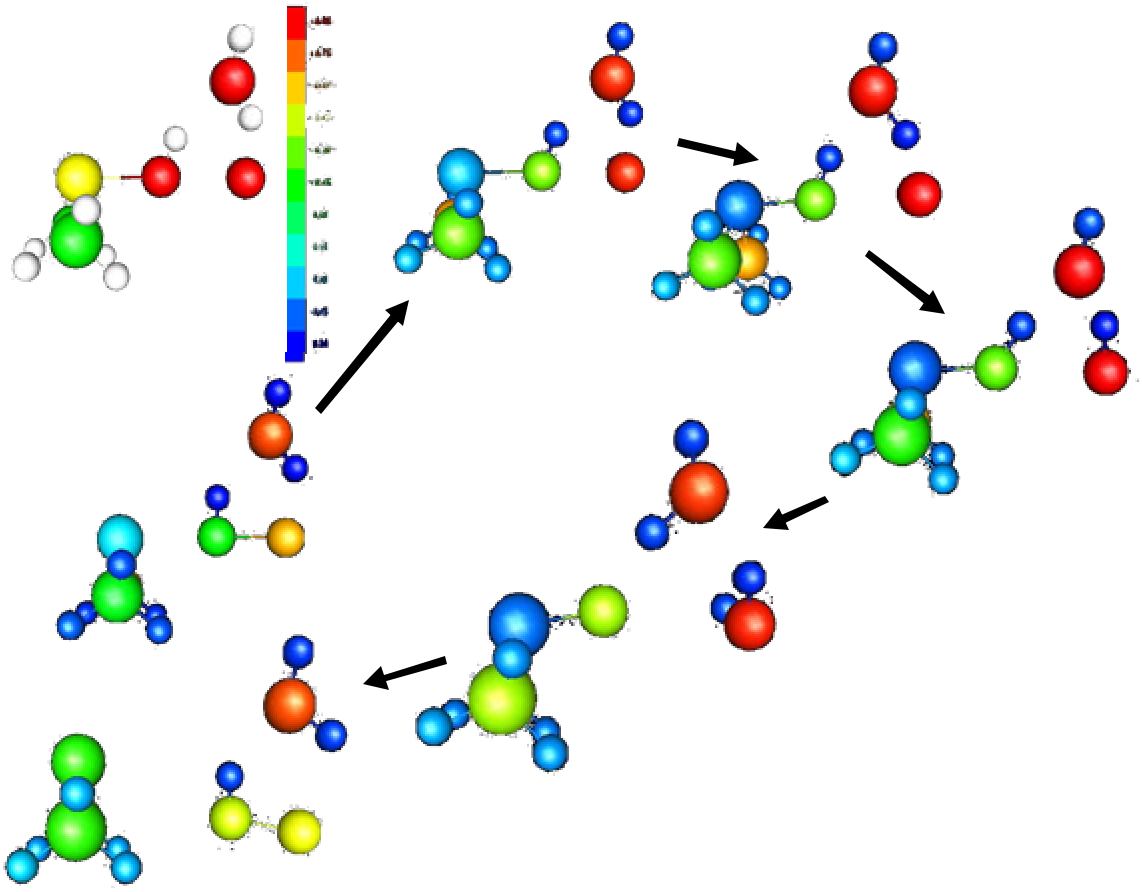

Fig. 2. Oxidation mechanism of dimethyl sulfide, an organic analog of proteins.

These results imply first that the current mechanism in the literature, that depicted in Equation (2) is not correct, and second that specific interactions of water (solvent) molecules with the hydrogen peroxide are important.

Figure 3 demonstrates the way in which pseudo first order rate constants were determined from the experimental data.

The concentration of each methionine residue was measured as a function of reaction time and plotted on a semi-log plot.

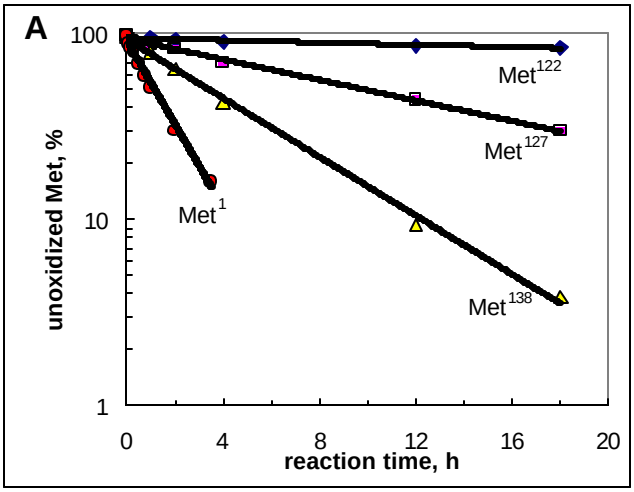

Fig. 3. Pseudo first order rate constants

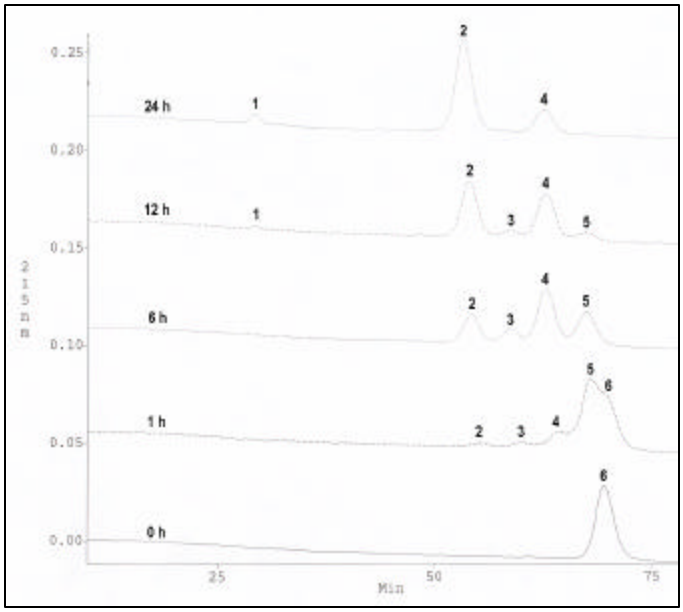

Fig. 4. HPLC curves used to determine the concentration of both oxidized and unoxidized amino acid residues.

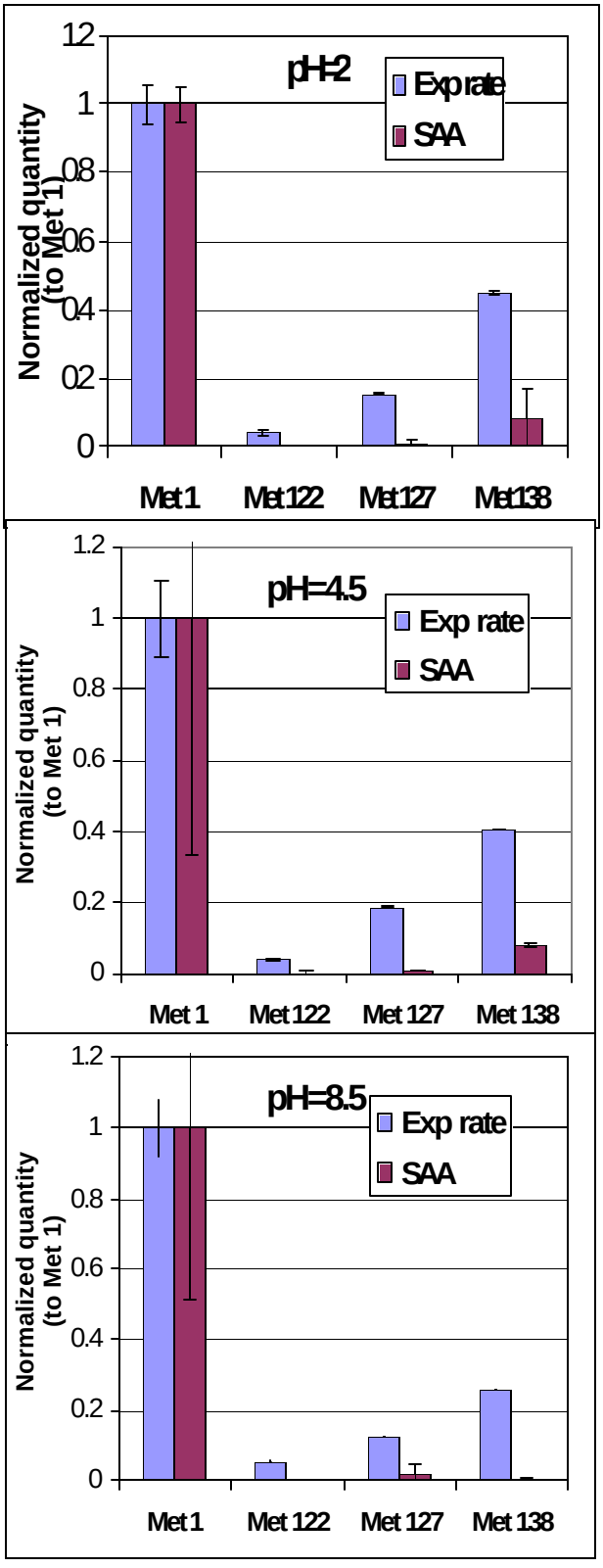

Fig. 5. Normalized rate of oxidation of methionine residues in G-CSF as a function of pH and compared to the solvent accessible area (SAA).

The pseudo first order rate constant is equal to the slope of this curve. The concentration of oxidized and unoxidized residues was determined using HPCL as shown in Fig. 4.

Fig. 5. demonstrates a correlation between a molecular-level property, solvent accessible area (SAA) in this case and normalized rates of oxidation. While there is qualitative agreement, there is not quantitative agreement. We are currently studying other properties and have found at least one that provides semi-quantitative agreement

Fig. 6 shows that there can be up to over a factor of two variation in the oxidation rate as a function of pH. Such as result demonstrates that pH can be used as an adjustable parameter in the stabilization of proteins.

IV. CONCLUSION

We have used quantum mechanical methods in order to demonstrate the proper mechanism of oxidation of methionine residues in proteins by studying simple organic analogs. We have also used molecular simulation methods on explicit models of proteins to develop an understanding of the molecular-level properties that contribute to protein oxidation. These we have validated using experimental methods.

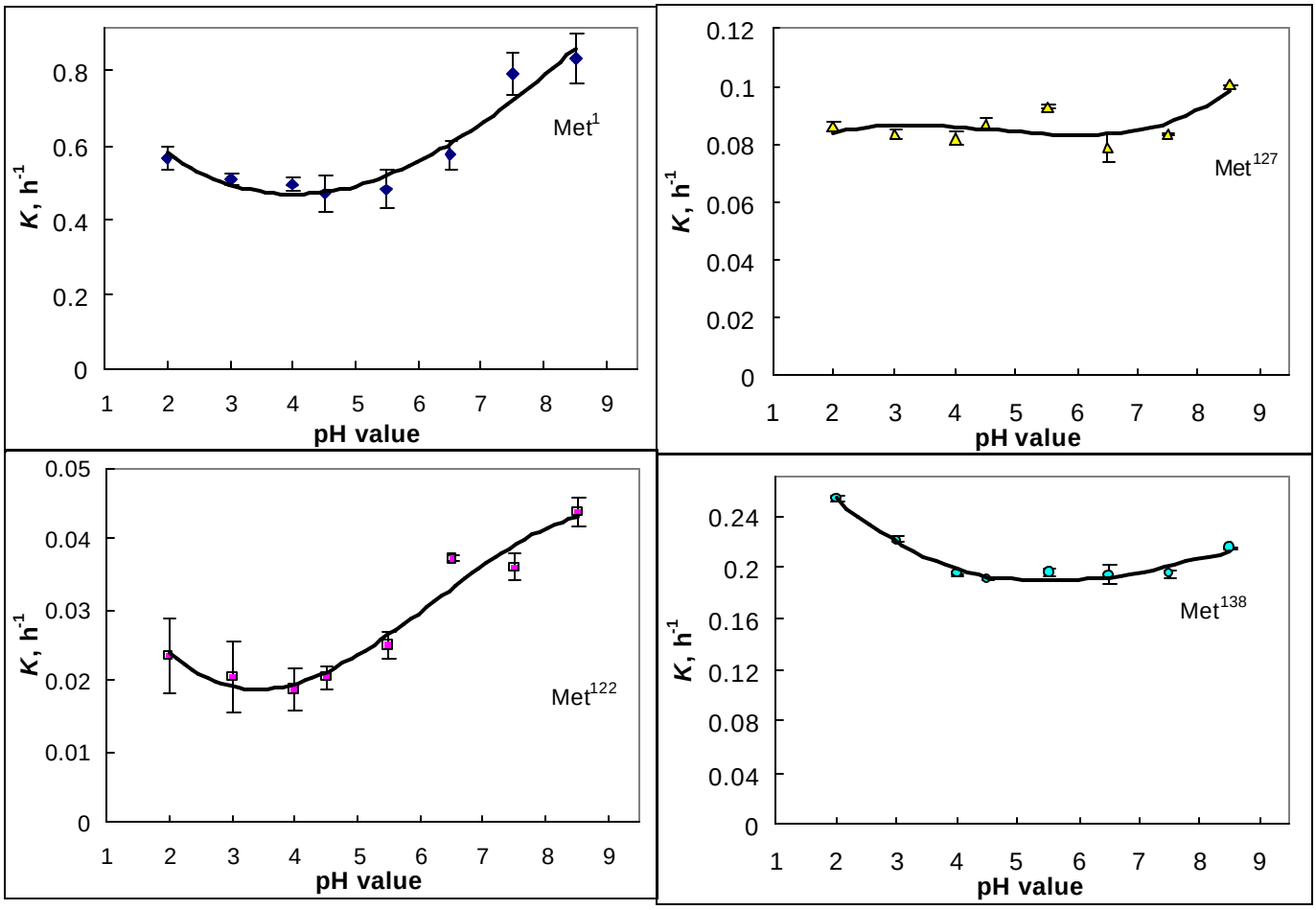

Fig. 6. Experimental pseudo-first order rate constants as a function of pH.

REFERENCES

[1] Carey, F. A. Organic Chemistry; 2nd ed.; McGraw-Hill Inc.: New York, 1992.

[2] Stadtman, E. R. Science 1992, 257, 1220-1224.

[3] John, O. E. In Peroxide Reaction Mechanisms; John, O. E., Ed.; Onterscience Publishers, Inc.: NewYork, 1960, pp 67-106.

[4] Cleland, J. L.; Powell, M. F.; Shire, J. Critical Reviews in Therapeutic Drug Carrier Systems 1993, 10, 307-377.

[5] Wang, W. Int. J. Pharm. 1999, 185, 129-188.

[6] Meyer, D. J.; Ho, B.; Manning, C. M. In Rational Design of Stable Protein Formulations Theory and Practice; Carpenter, F. J., Manning, C. M., Eds.; Kluwer Academic/Plenum Publishers: New York, 2002.

[7] Dankleff, M. A. P.; Ruggero, C.; Edwards, J. O.; Pyun, H. Y. J. Am. Chem. Soc. 1968, 90, 3209.

[8] Behrman, E. J.; John, O. E. Progr. Phys. Org. Chem. 1967, 4, 93.

[9] Curci, R.; DiPrete, R. A.; Edwards, J. O.; Mondena, G. J. J. Org. Chem. 1970, 35, 740.

[10] Bach, R. D.; Owensby, A. L.; Gonzalez, C.; Schlegel, H. B.; McDouall, J. J. W. J. Am. Chem. Soc. 1991, 113, 6001-6011.

[11] Bach, R. D.; Su, M. D.; Schlegel, H. B. J. Am. Chem. Soc. 1994, 116, 5379-5391.

[12] Dankleff, M. A. P.; Curci, R.; John, O. E.; Pyun, H.-Y. J. Am. Chem. Soc. 1967, 90, 3209.

[13] Bateman, L.; Hargrave, K. R. Proc. Roy. Soc. (London) 1954, A224, 389, 399.

[14] Okajima, T. Journal of Molecular Structure (Theochem) 2001, 572, 45-52.

[15] Ottolina, G.; Carrea, G. Chem. Commun. 2001, 1748-1749.

[16] Amels, R.; Elias, H.; Wannowius, K.-J. J. Chem. Soc. Faraday Trans. 1997, 93, 2537-2544.

[17] Nabichi, Y.; Fujiwara, E.; Kuboniwa, H.; Asoh, Y.; Ushio, H. Anal. chim. acta 1998, 365, 301-307.

[18] Frisch, M. J.; Trucks, G. W.; Schlegel, H. B.; Scruseria, G. E.; Robb, M. A.; Cheeseman, J. R.; Zakrzewski, V. G.; Montgomery, J. A.; Stratmann, R. E.; Burant, J. C.; Dapprich, S.; Millam, J. M.; Daniels, A. D.; Kudin, K. N.; Straion, M. C.; Farkas, O.; Tomasi, J.; Barone, V.; Cossi, M.; Cammi, R.; Mennucci, B.; Pomelli, C.; Adamo, C.; Clifford, S.; Ochterski, J.; Petersson, G. A.; Ayala, P. Y.; Cui, Q.; Morokuma, K.; Malick, D. K.; Rabuck, A. D.; Raghavachari, K.; Forseman, J. B.; Cioslowski, J.; Ortiz, J. V.; Stefanov, B. B.; Liu, G.; Liasenko, A.; Piskorz, P.; Komaromi, I.; Gomperts, R.; Martin, R. L.; Fox, D. J.; Keith, T.; Al-Laham, M. A.; Peng, C. Y.; Nanayakkara, A.; Gonzalez, C.; Challacombe, M.; Gill, P. M. W.; Johnson, B. G.; Chen, W.; Wong, M. W.; Andres, J. L.; Head-Gordon, M.; Replogle, E. S.; Pople, J. A.; Gaussian, Inc.: Pittsburgh, PA, 1998.

[19] Berke, A. D. J. Chem. Phys. 1993, 98, 5678.

[20] Scott, A. P.; Radom, L. J. Phys. Chem. 1996, 100, 16502-16513.

[21] MIERTUŠ, S.; Scrocco, E.; Tomasi, J. Chem. Phys. 1981, 55, 117-129.

[22] MIERTUŠ, S.; Tomasi, J. Chem. Phys. 1982, 65, 239-245.

[23] Barone, V.; Cossi, M.; Tomasi, J. J. chem. phys. 1997, 107, 3210-3221.

[24] Frisch, M. J.; Head-Gordon, M.; Pople, J. A. Chem. Phys. Lett. 1990, 166, 281.

[25] Frisch, M. J.; Head-Gordon, M.; Pople, J. A. Chem. Phys. Lett. 1990, 166, 275.

[26] Scuseria, G. E.; H. H. Schaefer, I. J. Chem. Phys. 1989, 90, 3700.

[27] Purvis, G. D.; Bartlett, R. J. J. Chem. Phys. 1982, 76, 1910.